Open
ORIGINAL ARTICLE

Cell Research (2015) 25:997-1012.
www.nature.com/cr

A miR-130a-YAP positive feedback loop promotes organ size and tumorigenesis

Shuying Shen[1, 2, *], Xiaocan Guo[1, *], Huan Yan[1], Yi Lu[4], Xinyan Ji[1], Li Li[5], Tingbo Liang[3], Dawang Zhou[6], Xin-Hua Feng[1], Jonathan C Zhao[7], Jindan Yu[7], Xing-Guo Gong[2], Lei Zhang[4], Bin Zhao[1]

[1]Life Sciences Institute and Innovation Center for Cell Signaling Network; [2]Institute of Biochemistry, College of Life Science; [3]Department of Hepatobiliary and Pancreatic Surgery and the Key Laboratory of Cancer Prevention and Intervention, The Second Affiliated Hospital, School of Medicine, Zhejiang University, Hangzhou, Zhejiang 310058, China; [4]State Key Laboratory of Cell Biology and Innovation Center for Cell Signaling Network, Institute of Biochemistry and Cell Biology, Shanghai Institutes for Biological Sciences, Chinese Academy of Sciences, Shanghai 200031, China; [5]Institute of Aging Research, Hangzhou Normal University, Hangzhou, Zhejiang 311121, China; [6]State Key Laboratory of Cellular Stress Biology, Innovation Center for Cell Signaling Network, School of Life Sciences, Xiamen University, Xiamen, Fujian 361102, China; [7]Department of Medicine, Division of Hematology/Oncology, Northwestern University Feinberg School of Medicine, Chicago, IL 60611, USA

Organ size determination is one of the most intriguing unsolved mysteries in biology. Aberrant activation of the major effector and transcription co-activator YAP in the Hippo pathway causes drastic organ enlargement in development and underlies tumorigenesis in many human cancers. However, how robust YAP activation is achieved during organ size control remains elusive. Here we report that the YAP signaling is sustained through a novel microRNA-dependent positive feedback loop. miR-130a, which is directly induced by YAP, could effectively repress VGLL4, an inhibitor of YAP activity, thereby amplifying the YAP signals. Inhibition of miR-130a reversed liver size enlargement induced by Hippo pathway inactivation and blocked YAP-induced tumorigenesis. Furthermore, the *Drosophila* Hippo pathway target *bantam* functionally mimics miR-130a by repressing the VGLL4 homolog SdBP/Tgi. These findings reveal an evolutionarily conserved positive feedback mechanism underlying robustness of the Hippo pathway in size control and tumorigenesis.

***Keywords*:** microRNA; YAP; Hippo; tumorigenesis; organ size
Cell Research (2015) **25**:997-1012. doi:10.1038/cr.2015.98; published online 14 August 2015

Introduction

A predetermined relative organ size is one of the most visible features distinguishing multicellular species. However, the underlying mechanism remains enigmatic. Identification of the Hippo pathway shed some light on this problem. Genetic manipulation of Hippo pathway genes leads to drastic change of organ size in *Drosophila* and mammals [1, 2]. For instance, liver-specific expression of *Yes-associated protein* (*YAP*) transgene, the major effector of the Hippo pathway, leads to striking enlargement of liver up to one fourth of mouse body weight [3]. In addition, the Hippo pathway also regulates regeneration of organs such as heart and intestine [4-6]. Thus, Hippo signaling is important for both developmental size control and tissue homeostasis.

Intensive investigations have delineated hierarchy of the Hippo pathway in which the mammalian Mst1/2 kinases (*Drosophila* Hippo homologs) in complex with a scaffold protein Sav1, phosphorylate and activate the Lats1/2 kinases (*Drosophila* Wts homologs) [7, 8] that are associated with the scaffold protein Mob1 [9]. Lats1/2 phosphorylate YAP and its paralog transcriptional co-activator with PDZ-binding motif (TAZ, YAP and TAZ are *Drosophila* Yki homologs), thereby inhibiting YAP and TAZ by inducing their cytoplasmic translocation

*These two authors contributed equally to this work.
Tel: 86-571-8820-8545; Fax: 86-571-8898-1336
Correspondence: Bin Zhao
E-mail: binzhao@zju.edu.cn
Received 18 April 2015; revised 24 June 2015; accepted 30 June 2015; published online 14 August 2015

and degradation [10-14]. YAP and TAZ are transcription co-activators activating gene expression largely through interaction with TEAD (homolog of *Drosophila* Scalloped, Sd) family and other transcription factors [15-17]. It was recently discovered that extracellular signaling molecules such as lysophosphatidic acid regulate Hippo signaling by binding to their cell surface G-protein-coupled receptors, which in turn transduce the signal to the actin cytoskeleton, thus inhibiting Lats1/2 through a yet unclear mechanism [18, 19]. Interestingly, mechanical stresses such as matrix stiffness and cell adhesion status also regulate the Hippo pathway through the actin cytoskeleton [20-23]. This is consistent with the described role of adhesion and polarity genes acting as potent regulators of organ size [24].

Consistent with its anti-apoptotic, pro-proliferative and stemness-promoting activities, YAP is highly tumorigenic once unleashed from inhibition by the Hippo pathway. It not only promotes cancerous traits in cultured cells but also potently induces tumorigenesis in multiple organs [3, 10, 17, 25-27]. In human cancers, YAP is activated by genomic amplification [28, 29] and deregulation of the Hippo pathway. For example, the Hippo pathway upstream component *NF2* is a *bone fide* tumor suppressor mutated in neurofibromatosis 2, and activating mutations of $G_{q/11}$, upstream inhibitors of the Hippo pathway, are the leading cause of uveal melanoma. YAP activation had been shown to be critical for these cancers [30-32]. Interestingly, the tumorigenic potential of YAP was recently found inhibited by VGLL4, a potential tumor suppressor competing for TEAD binding [33-35]. It is currently unclear if the Hippo pathway and VGLL4 coordinate for YAP inhibition or if they are mechanistically independent.

MicroRNAs are small noncoding RNAs that regulate protein expression post-transcriptionally through repression of mRNA stability or translation. The *Drosophila* Hippo pathway inhibits transcription of a microRNA *bantam* that plays an important role in regulation of cell proliferation, apoptosis, stem cell self-renewal and organ size [36-38]. However, *bantam* is not conserved in mammals and a mammalian functional counterpart of *bantam* is elusive. Here we report that YAP directly induces expression of miR-130a, which in turn represses the protein level of VGLL4, thus forming a YAP-miR-130a-VGLL4 positive feedback loop amplifying upstream signals. Furthermore, miR-130a inhibition markedly reversed organ size enlargement and tumorigenesis induced by aberrant YAP activation. Interestingly, *bantam* directly targets SdBP/Tgi, the *Drosophila* homolog of VGLL4; thus, it is analogous to miR-130a. These findings uncover a key mechanism underlying robust increase of organ size upon Hippo pathway inactivation and tumorigenesis induced by YAP activation. Our studies also suggest miR130 inhibition as a new approach to target YAP in cancer.

Results

miR-130a mediates the oncogenic potential of YAP

Profiling of Hippo pathway target genes in mammalian cells or tissues has not yet revealed the key mediator of size regulation and tumorigenesis *in vivo* [3, 10, 12]. To examine whether microRNAs may mediate YAP functions we profiled YAP-induced microRNAs in MCF10A cells by microarray (Figure 1A). Validation of the hits showed that miR-130a was one of the best-induced microRNAs by YAP (Figure 1B and Supplementary information, Figure S1A). More importantly, knockdown of endogenous YAP and TAZ substantially reduced pri- and mature miR-130a levels in multiple cell lines (Figure 1C and Supplementary information, Figure S1B).

To investigate the role of *miR-130a* as a YAP target gene, we examined its function in YAP-induced overgrowth and oncogenic transformation. Interestingly, inhibition of miR-130a by microRNA sponge hampered overgrowth induced by the Hippo pathway-resistant YAP-5SA mutant [11] (Figure 1D). Consistently, expression of miR-130a cooperated with YAP-S127A mutant, which is resistant to Hippo pathway-induced cytoplasmic translocation, to promote cell proliferation (Figure 1D). Remarkably, inhibition of miR-130a also strongly suppressed YAP-5SA-induced anchorage-independent growth, a hallmark of oncogenic transformation (Figure 1E). Compared with HepG2 cells, the induction of miR-130a by YAP-5SA is lower in HMLE cells (Figure 1B). Therefore, we investigated whether further increase of miR-130a level would cooperate with YAP to promote transformation of HMLE cells. Indeed, although expression of miR-130a alone was unable to transform cells, it cooperated with YAP-5SA to promote colony formation (Figure 1F). Furthermore, miR-130a promoted tumorigenesis induced by YAP-S127A in HepG2 cells (Figure 1G). Expression of miR-130a alone could not induce tumor growth from HepG2 cells (data not shown). Moreover, expression of the miR-130a sponge inhibited tumor formation induced by YAP-S127A in HepG2 cells (Figure 1H and Supplementary information, Figure S1C). Thus, *miR-130a* is a YAP target gene important for over-proliferation and tumorigenesis *in vitro* and *in vivo*.

miR-130a is a direct target of YAP-TEAD

To determine how YAP induces miR-130a, we checked whether the induction depends on TEADs. Indeed, mutation of YAP serine 94 (S94), a residue critical

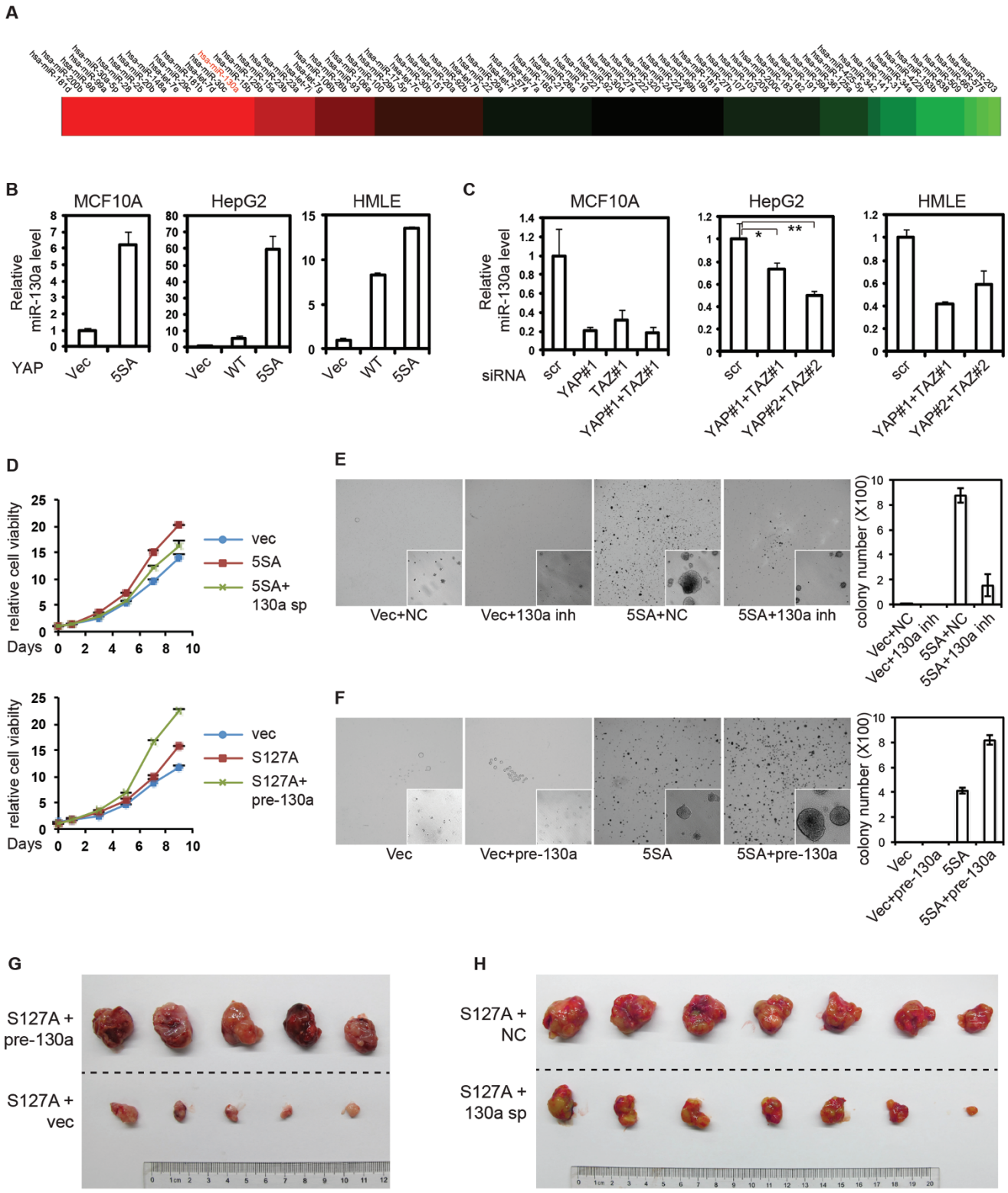

Figure 1 miR-130a mediates the oncogenic potential of YAP. **(A)** YAP-regulated microRNAs. microRNAs regulated by YAP were determined by microRNA microarrays. microRNAs with a *P*-value of < 0.01 in ectopic YAP-expressing MCF10A cells and a signal of more than 500 in control cells were selected and the heatmap was drawn using Matlab. **(B, C)** YAP induces *miR-130a* expression. MicroRNAs were extracted and *miR-130a* expression levels were determined by quantitative RT-PCR. Experiments were performed in triplicates. * and ** indicate a *P*-value of < 0.05 and < 0.01, respectively, as calculated

by student's *t*-test. **(D)** miR-130a plays a role in YAP-induced cell proliferation. Pre-miR-130a or the miR-130a sponge was expressed with YAP-S127A or YAP-5SA in HepG2 stable cells. Cell viability was determined by CellTiter-Blue assay. **(E**, **F)** miR-130a in cellular transformation induced by YAP-5SA. Vector (Vec) or YAP-5SA-expressing HepG2 stable cells transfected with negative control (NC) or miR-130a inhibitor **(E)** or HMLE stable cells infected with empty vector or YAP-5SA with or without pre-miR-130a **(F)** were cultured in soft agar for 20 days. Colonies were stained with crystal violet, photographed and quantified by ImageJ (details are shown in inserts). **(G** and **H)** miR-130a in YAP-induced tumorigenesis *in vivo*. Nude mice were injected on the two flanks with 6×10^6 **(G)** or 1×10^7 **(H)** HepG2 stable cells. Tumors were dissected after 3 **(G)** or 4 **(H)** weeks and were photographed.

for TEAD interaction [15], abrogated miR-130a induction (Figure 2A). Furthermore, knockdown of TEADs strongly reduced miR-130a expression (Figure 2B and Supplementary information, Figure S2A, S2B). To confirm the regulation of miR-130a activity by YAP-TEAD, we constructed a miR-130a sensor fusing a stretch of four perfect miR-130a binding sites 3′ to the luciferase gene. Function of the sensor was confirmed by co-transfection with miR-130a mimic and inhibitor (Supplementary information, Figure S2C). Indeed, YAP but not the S94A mutant clearly repressed miR-130a sensor activity (Figure 2C). Thus miR-130a is a target of YAP-TEAD transcriptional complex.

To determine how YAP-TEAD activates miR-130a expression, we dissected the *miR-130a* promoter (Figure 2D). The transcription start site of pri-miR-130a was first predicted by the miRStart tool and then confirmed by RT-PCR (Supplementary information, Figure S2D). YAP binding to *miR-130a* promoter was then examined by chromatin immunoprecipitation (ChIP). Immunoblotting indicated efficient immunoprecipitation of Flag-YAP-5SA (Supplementary information, Figure S2E) and PCR revealed that YAP bound largely to the −2 000 to 0 bp proximal promoter of *miR-130a* (Figure 2E). Consistently, ChIP of endogenous YAP and TEAD1 showed binding not only to *CTGF* promoter as previously reported [15], but also to *miR-130a* promoter (Figure 2F, Supplementary information, Figure S2F). Furthermore, YAP and TEAD2 activated a *miR-130a* promoter reporter in a manner dependent on TEAD-binding site (TB) 1 and TB2 but not other potential TBs (TB3/4 and data not shown; Figure 2G). Notably, the organization and position of TB1/2 sites on *miR-130a* promoter is highly similar to that on *CTGF* promoter [15]. These studies demonstrate that *miR-130a* is a direct target gene of YAP and TEAD.

miR-130a represses VGLL4

To dissect how miR-130a functions downstream of YAP, we used the Targetscan algorithm to predict potential miR-130a targets (Supplementary information, Table S1). Interestingly, one of the hits was VGLL4, a known YAP inhibitor. In line with miR-130a as a vertebrate-specific microRNA, a miR-130a seed-binding site in *VGLL4* 3′UTR is conserved in vertebrates, suggesting its functional importance (Figure 3A). To determine the functionality of this predicted site, we constructed a *VGLL4* 3′UTR sensor. Despite substantial repression and activation of the wild-type (WT) sensor by miR-130a mimic and inhibitor, respectively, the seed-matching region mutant sensor remained unresponsive (Figure 3B). Therefore, miR-130a could specifically bind to *VGLL4* 3′UTR. Furthermore, transfection of miR-130a mimic or expression of pre-miR-130a substantially repressed endogenous VGLL4 protein level (Figure 3C, 3D) as indicated by a validated antibody (Supplementary information, Figure S3A). More importantly, inhibition of endogenous miR-130a by an inhibitor antisense oligomer or microRNA sponge clearly increased VGLL4 protein level in multiple cell lines from different tissue origins (Figure 3E, 3F). However, miR-130a did not significantly alter VGLL4 mRNA level (Supplementary information, Figure S3B), suggesting a mechanism of translation repression. In support of the functional importance of VGLL4 as a miR-130a target, miR-130a-induced cell proliferation was blocked by VGLL4 overexpression (Figure 3G). Furthermore, knockdown of VGLL4 rescued cell proliferation defects caused by miR-130a inhibition (Figure 3G). Taken together, VGLL4 is a miR-130a target critical for growth regulation.

miR-130a activates YAP by repressing VGLL4

VGLL4 is a repressor of YAP activity through competition for TEAD binding. Therefore, by repressing VGLL4, the YAP target gene *miR-130a* could potentially act as an activator of YAP. Indeed, expression of miR-130a activated a *CTGF* reporter, a well-defined readout of YAP transcriptional activity (Figure 4A and Supplementary information, Figure S4A). However, co-expression of miR-130a-insensitive VGLL4 from constructs lacking the 3′UTR normalized the reporter activity dose-dependently (Figure 4A). More importantly, inhibition of miR-130a attenuated *CTGF* reporter activity in a VGLL4-dependent manner (Figure 4B and Supplementary information, Figure S4A), suggesting that YAP is regulated by endogenous miR-130a through VGLL4.

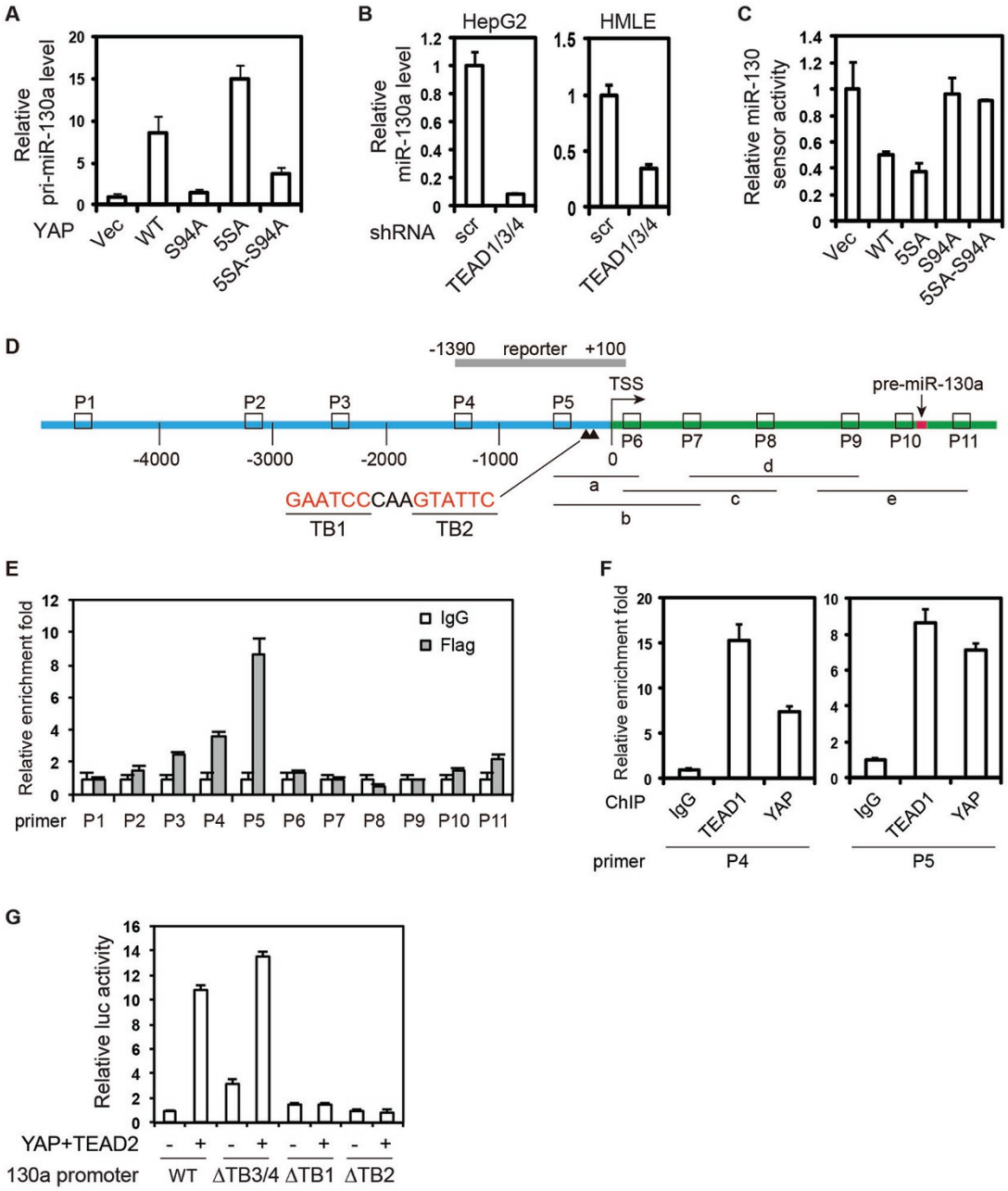

Figure 2 *miR-130a* is a direct target gene of YAP-TEAD. **(A)** YAP induces *miR-130a* expression in an S94-dependent manner. pri-miR-130a expression levels in indicated MCF10A stable cells were determined by quantitative RT-PCR. Experiments were performed in triplicates. **(B)** Knockdown of TEADs reduces miR-130a level. Cells were infected with the shRNA targeting TEAD1/3/4. The levels of mature miR-130a were determined. Experiments were performed in triplicates. **(C)** YAP represses miR-130a sensor activity in an S94-dependent manner. HepG2 cells were transfected with miR-130a sensor and YAP WT or mutants for luciferase assay. Experiments were performed in duplicates. **(D)** *miR-130a* genomic structure. *miR-130a* promoter is in blue, pri-miR-130a encoding region is in green, and pre-miR-130a encoding region is in red. Regions amplified by ChIP-PCR primers are labeled as P1 to P11. Regions amplified by primers used in RT-PCR confirmation of TSS are labeled as a-e. The proximal promoter cloned for luciferase reporter is indicated. **(E**, **F)** YAP and TEAD bind to the proximal promoter of *miR-130a*. HepG2 cells expressing Flag-YAP-5SA **(E)** or native HepG2 cells **(F)** were processed for ChIP with control IgG or antibodies against TEAD1 and YAP followed by quantitative PCR. Experiments were performed in duplicates. **(G)** YAP activates *miR-130a* promoter reporter in a TEAD-dependent manner. WT or mutant *miR-130a* reporters were transfected with or without YAP and TEAD2 into HEK293T cells for luciferase assay. Experiments were performed in duplicates.

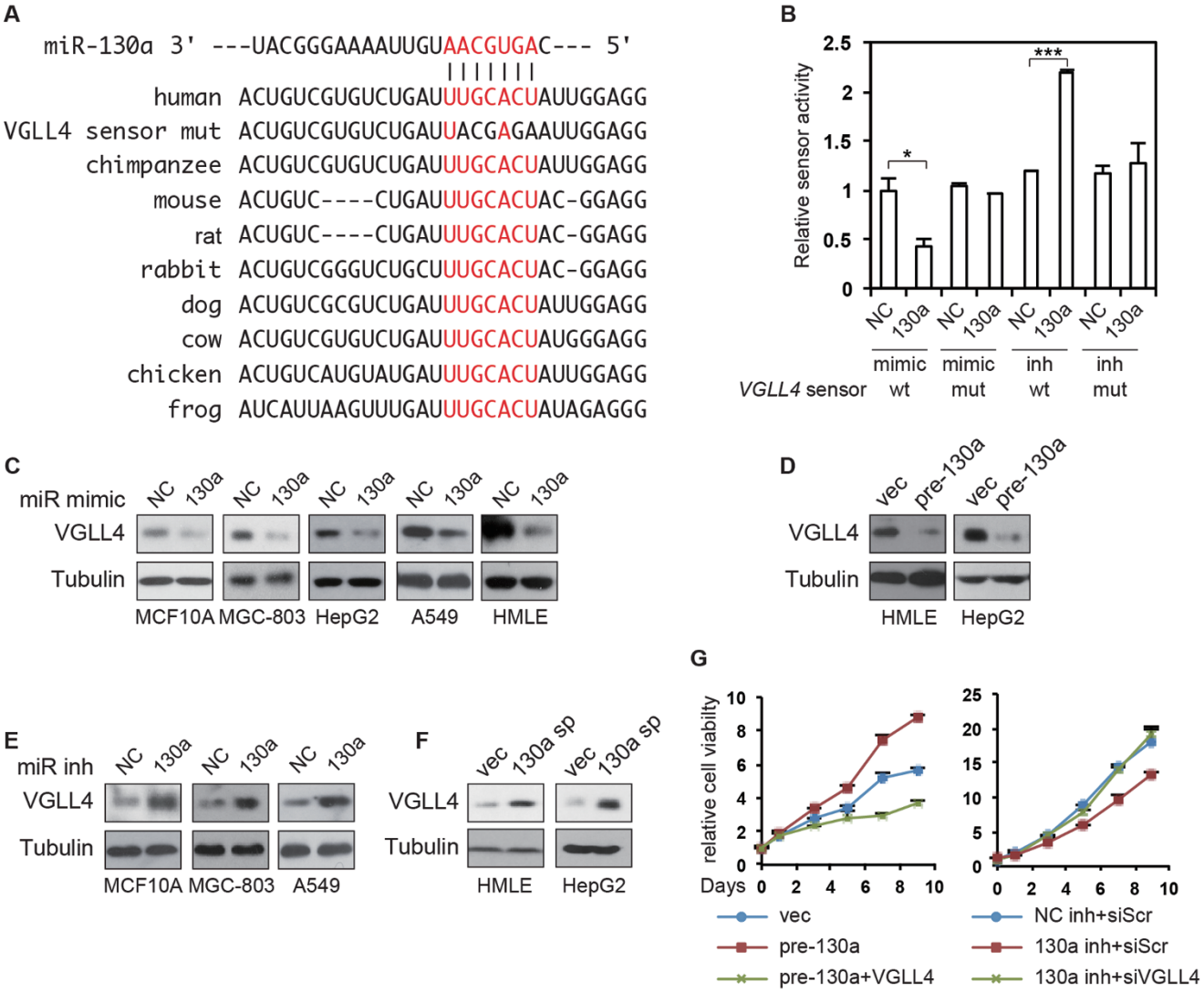

Figure 3 miR-130a represses VGLL4. **(A)** Conservation of miR-130a binding sites in *VGLL4* 3′UTR in vertebrates. *VGLL4* 3′UTR from different species are aligned together with miR-130a. The seed region and its matching nucleotides are in red. Base paring is indicated by a line. Mutation of *VGLL4* 3′UTR sensor is also shown. **(B)** miR-130a regulates *VGLL4* sensor activity. HEK293T cells were transfected with WT or mutant *VGLL4* 3′UTR sensor together with miR-130a mimic or inhibitor. Sensor activities were determined by luciferase assay. Experiments were performed in duplicates. * and *** indicate a *P*-value of < 0.05 and < 0.001, respectively, as calculated by student's *t*-test. **(C, D)** miR-130a represses VGLL4 protein level. Cells were transfected with NC or miR-130a mimic **(C)** or infected with empty vector or pre-miR-130a **(D)**. Cell lysates were subjected to immunoblotting. **(E, F)** miR-130a inhibition increases VGLL4 protein level. Cells were transfected with NC or miR-130a inhibitor **(E)** or infected with empty vector or the miR-130a sponge **(F)** and analyzed for VGLL4 protein level. **(G)** miR-130a promotes cell proliferation by repressing VGLL4. Cells were transduced with pre-miR-130a and VGLL4 (left panel, HMLE cells) or transfected with miR-130a inhibitor and VGLL4 siRNA (right panel, HepG2 cells) as indicated. Cell viability was determined by CellTiter-Blue assay.

Furthermore, expression of YAP target genes *CTGF* and *Cyr61* was enhanced or repressed by activation or inhibition of miR-130a, respectively (Supplementary information, Figure S4B, S4C, S4D). Consistently, VGLL4 overexpression or YAP and TAZ knockdown (Supplementary information, Figure S4E, S4F) blocked YAP target gene induction by miR-130a mimic (Figure 4C, 4D), while knockdown of VGLL4 (Supplementary information, Figure S4G) rescued YAP target gene expression in the presence of miR-130a inhibitor (Figure 4E). Thus, miR-

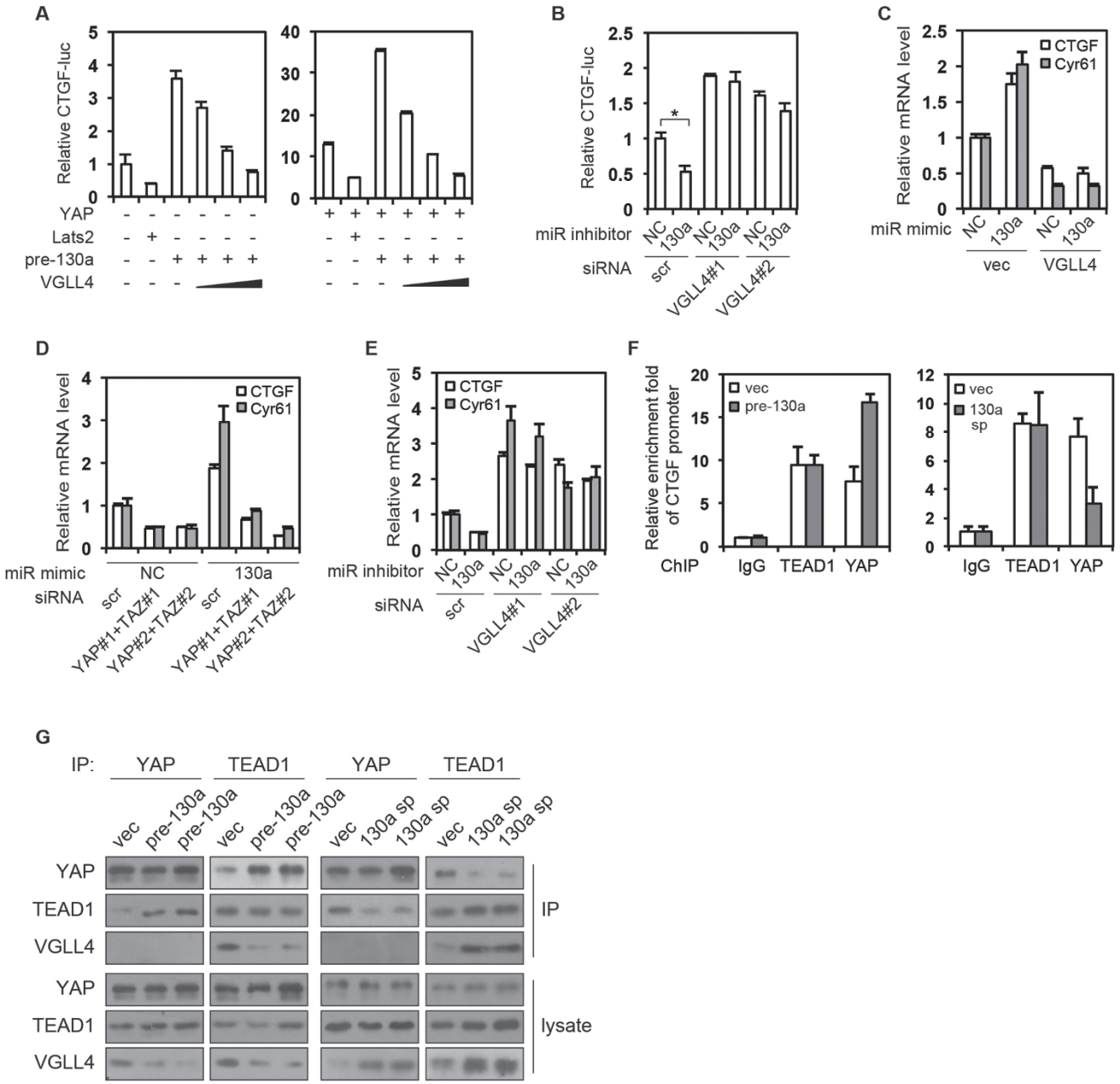

Figure 4 miR-130a activates YAP through repression of VGLL4. **(A)** miR-130a activates YAP transcriptional activity. *CTGF*-luciferase reporter was co-transfected with other plasmids into HEK293T cells as indicated for luciferase assay. Experiments were performed in duplicates. **(B)** miR-130a inhibition suppresses YAP transcriptional activity in a VGLL4-dependent manner. HEK293T cells stably expressing *CTGF*-luciferase reporter were transfected as indicated for luciferase assay. Experiments were performed in duplicates. * indicates a *P*-value of < 0.05 as calculated by student's *t*-test. **(C)** miR-130a promotes YAP target gene expression, which is blocked by VGLL4. Control or VGLL4-overexpressing HepG2 cells were transfected with NC or miR-130a mimic for gene expression analysis. Experiments were performed in triplicates. **(D)** miR-130a promotes Hippo pathway target gene expression in a YAP-and-TAZ-dependent manner. HepG2 cells were transfected as indicated for gene expression assay. Experiments were performed in triplicates. **(E)** miR-130a inhibition suppresses YAP target gene expression in a VGLL4-dependent manner. HMLE cells were transfected and gene expression was determined. Experiments were performed in triplicates. **(F)** miR-130a regulates YAP binding to target gene promoter. ChIP was performed using control IgG or antibodies against TEAD1 and YAP on HepG2 stable cell lysates. Relative enrichment of *CTGF* promoter was determined by quantitative PCR in triplicates. **(G)** miR-130a regulates YAP-TEAD1 interaction. HepG2 cells stably expressing miR-130a precursor or sponge and respective empty vectors were lysed and immunoprecipitated with anti-YAP or anti-TEAD1 antibodies. Lysates and immunoprecipitates were analyzed by western blots.

130a promotes Hippo pathway transcriptional output by repressing VGLL4 protein level. Such a mechanism implies that YAP binding to target gene promoters would be regulated by miR-130a. Indeed, we observed an enhanced or suppressed binding of YAP to *CTGF* promoter by pre-miR-130a and the miR-130a sponge, respectively (Figure 4F). Notably, the binding of TEAD1 to *CTGF* promoter was not affected. The mechanism would also predict that miR-130a promotes the binding between YAP and TEADs. By immunoprecipitating endogenous YAP or TEAD1 from miR-130a precursor or sponge expressing cells we indeed observed that pre-miR130a inhibited VGLL4-TEAD1 interaction and promoted YAP-TEAD1 interaction while miR-130a sponge promoted VGLL4-TEAD1 interaction and repressed YAP-TEAD1 interaction (Figure 4G). Taken together, miR-130a is not only a Hippo pathway target but also an activator of YAP.

The YAP-miR-130a-VGLL4 positive feedback loop mediates Hippo signaling

The above data suggests the possibility of a YAP-miR-130a-VGLL4 positive feedback loop acting downstream of Hippo signaling to mediate potent responses to stimuli. Such a mechanism predicts the Hippo pathway in control of VGLL4 protein level. Indeed, knockdown of YAP and TAZ or TEADs substantially increased VGLL4 protein levels in cancer and noncancerous cell lines from various tissue origins (Figure 5A, 5B and Supplementary information, Figure S5A, S5B), suggesting widespread existence of the mechanism. However, VGLL4 mRNA level and protein stability were not affected by YAP and TAZ knockdown (Supplementary information, Figure S5C, S5D). Furthermore, overexpression of WT YAP or the WW domain mutant but not the S94A mutant repressed VGLL4 protein level (Supplementary information, Figure S5E). In support of that miR-130a is the underlying mechanism for VGLL4 regulation by YAP, miR-130a mimic abrogated VGLL4 induction by YAP and TAZ knockdown (Figure 5C), and miR-130a inhibition rescued VGLL4 expression upon YAP activation (Figure 5D and Supplementary information, Figure S5F). Thus YAP-TEAD actively represses VGLL4 level through miR-130a.

Through inhibition of YAP, the Hippo pathway kinases should be positive regulators of VGLL4 protein expression. Indeed, knockdown of Lats1/2 decreased VGLL4 protein level (Figure 5E). More importantly, while *Mst1/2* knockout increased liver size (Supplementary information, Figure S5G), the expression of miR-130a was substantially elevated and protein level of VGLL4 was diminished (Figure 5F and Supplementary information, Figure S5H). Thus the Hippo pathway regulates VGLL4 protein level *in vivo*, and the two mechanisms of YAP inhibition are therefore connected.

We then determined whether the YAP-miR-130a-VGLL4 positive feedback loop mediates Hippo pathway output in response to upstream signals such as cell suspension. In consistence with YAP inhibition as previously reported [20], cell suspension suppressed miR-130a level in a Lats1/2-dependent manner (Figure 5G and Supplementary information, Figure S5I), which could be rescued by YAP overexpression (Supplementary information, Figure S5J). Interestingly, we found much higher VGLL4 protein but not mRNA levels in cells cultured in suspension (Figure 5H and Supplementary information, Figure S5K). Importantly, ectopic expression of YAP or miR-130a restored a normal VGLL4 level in suspension cells (Figure 5H, 5I). Repression of YAP through the Hippo pathway is important for apoptosis upon cell detachment called anoikis. Interestingly, expression of pre-miR-130a repressed anoikis alone or in cooperation with YAP (Figure 5J). In contrast, inhibition of miR-130a enhanced anoikis in the liver cancer cell line HepG2, which is defective in anoikis under basal conditions (Figure 5K). These data suggest that upstream signals of the Hippo pathway such as cell suspension are amplified by a YAP-miR-130a-VGLL4 positive feedback loop to elicit functional responses such as anoikis.

miR-130a promotes YAP-induced tumorigenesis and enlargement of mouse liver

We further investigated the miR-130a-mediated positive feedback mechanism in mouse liver. Genetic inactivation of Hippo pathway components such as *Mst1/2*, *Sav* and *NF2* potently induces liver tumorigenesis [26, 32, 39-42]. However, except for *NF2*, germline mutations of these genes have not been reported in human cancer. This suggests that defects in this pathway in cancer are more commonly somatic and mosaic. To more accurately model this situation, we used the hydrodynamic injection method to deliver transposon plasmids encoding YAP and the *piggyBac* transposase, which led to stable mosaic YAP expression in hepatocytes (Figure 6A). Despite recent report using similar method suggesting that YAP-S127A alone was not tumorigenic [43], the YAP-5SA mutant induced large tumors 100 days post-injection (Figure 6B and Supplementary information, Figure S6A). This result indicates that aberrant YAP activation alone is sufficient to drive liver tumorigenesis in a normal tissue microenvironment. Obviously, the repression imposed on YAP by VGLL4 must be circumvented. Indeed, in YAP-induced tumors, the expression of miR-130a was elevated and VGLL4 protein but not mRNA level was

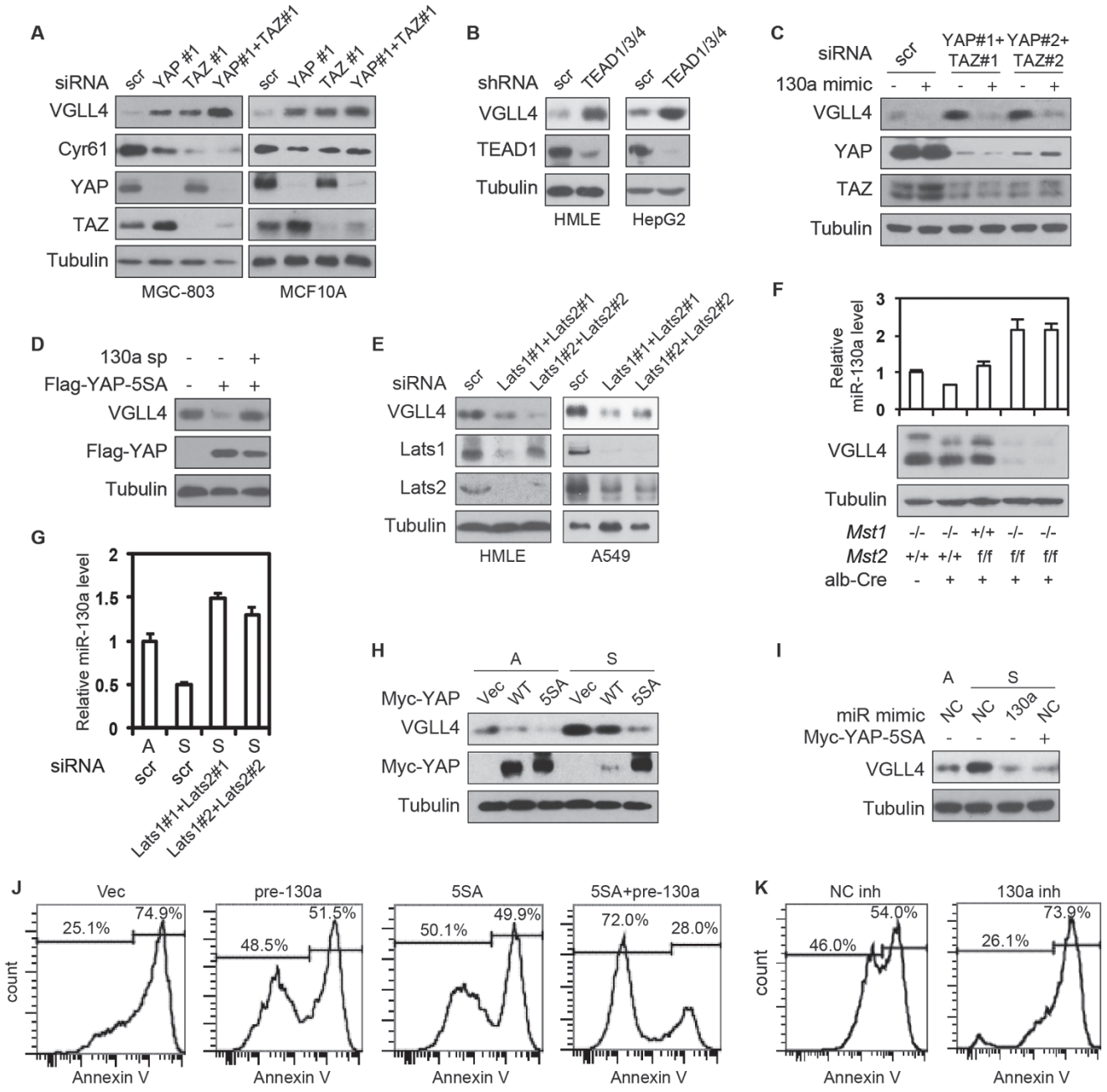

Figure 5 The YAP-miR-130a-VGLL4 positive feedback loop mediates Hippo signaling. **(A**, **B)** Knockdown of YAP, TAZ and TEADs increases VGLL4 protein level. Cells were transfected with siRNAs **(A)** or infected with shRNA **(B)** and analyzed by immunoblotting. Cyr61 is a known YAP target and a positive control. **(C)** miR-130a blocks VGLL4 induction upon YAP and TAZ inhibition in HMLE cells. **(D)** The miR-130a sponge abrogates VGLL4 inhibition by YAP in HepG2 cells. **(E)** Knockdown of Lats1/2 represses VGLL4 protein level. Cells were transfected with siRNAs as indicated and analyzed by immunoblotting. **(F)** Inactivation of the Hippo pathway *in vivo* increases miR-130a and represses VGLL4 protein level. Control and albumin-Cre-mediated *Mst1/2* conditional knockout livers were harvested at 2 months of age for analysis. **(G)** Loss of cell adhesion represses miR-130a in a Lats1/2-dependent manner. siRNA-transfected HMLE cells were cultured in adhesion "A" or in suspension "S" for 48 h for analysis of miR-130a level. **(H**, **I)** Cell suspension induces VGLL4 by inhibiting YAP and miR-130a. HMLE stable cells were transfected and cultured in adhesion or in suspension for 48 h and analyzed by immunoblotting. **(J)** miR-130a inhibits anoikis in cooperation with YAP. HMLE stable cells were subjected to suspension culture for 48 h. Anoikis rates were determined by Annexin V staining and FACS. **(K)** Inhibition of miR-130a promotes anoikis. HepG2 cells were transfected and analyzed as in **J**.

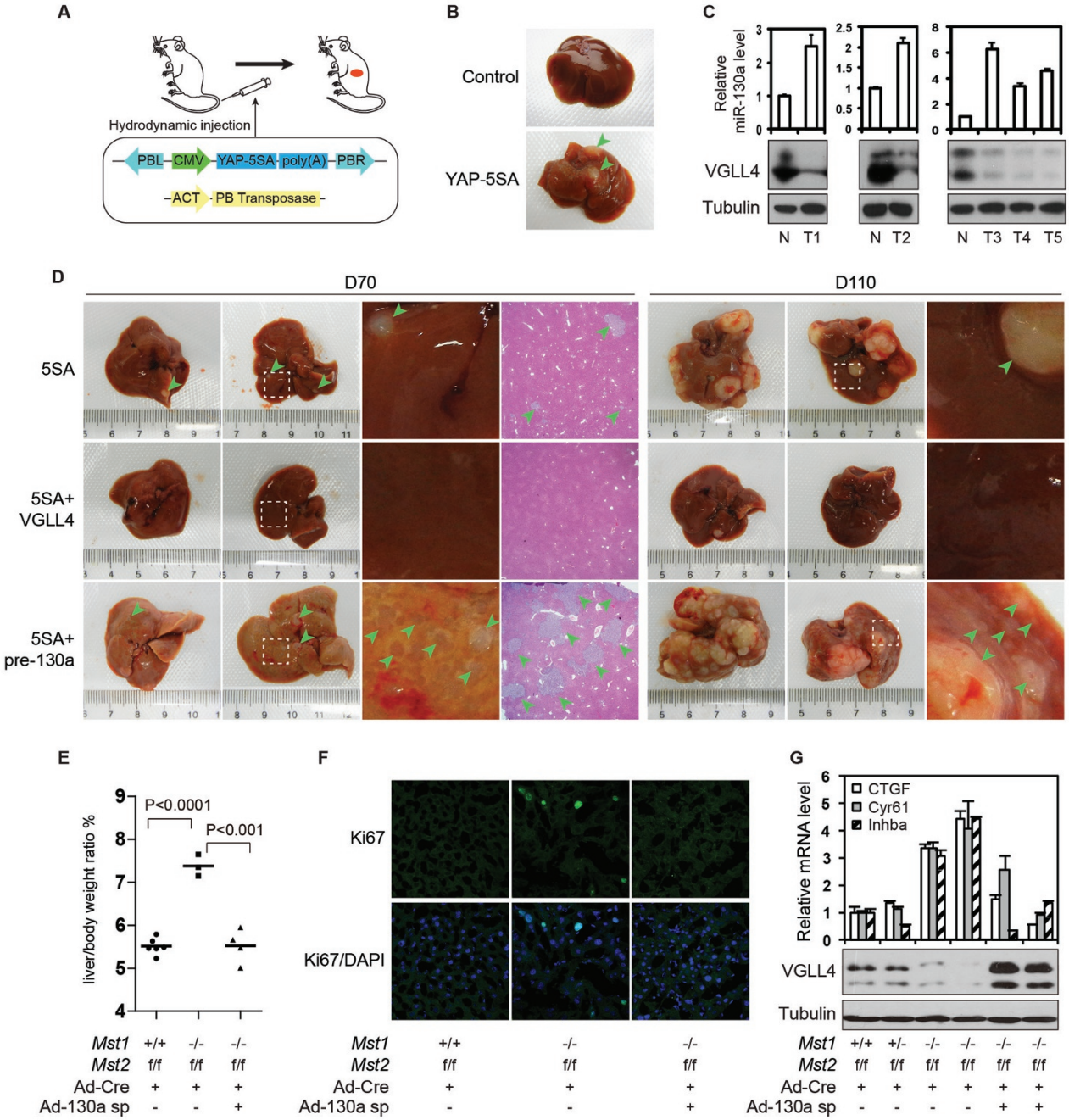

Figure 6 miR-130a in liver tumorigenesis and size control. **(A)** Schematic of liver tumorigenesis model by the hydrodynamic injection method. **(B)** YAP-5SA induces liver tumorigenesis. Control and YAP-5SA-injected livers 100 days post-injection are shown. Arrowheads indicate tumors. **(C)** Activation of miR-130a and inhibition of VGLL4 protein levels in YAP-induced liver tumors. YAP-5SA-induced tumors and adjacent normal tissues from 3 mice were processed for analysis. **(D)** YAP-induced tumorigenesis is repressed by VGLL4 and promoted by miR-130a. YAP-5SA was expressed alone or together with VGLL4 or pre-miR130a by hydrodynamic injection. Tumorigenesis was analyzed at 70 or 110 days after injection. Boxed areas are enlarged on the right. H&E-stained D70 liver sections are also shown. Green arrowheads indicate lesions. **(E**, **F)** miR-130a sponge abrogates liver enlargement **(E)** and hepatocyte proliferation **(F)** induced by *Mst1/2* knockout. Mice of the indicated genotypes were transduced with adenoviral Cre and miR-130a sponge as indicated. Mice were sacrificed 9 days after injection for liver/body weight ratios **(E)** and Ki67 staining (**F**, green). *P*-values were calculated by student's *t*-test. **(G)** miR-130a sponge abrogates VGLL4 repression and YAP target gene induction by *Mst1/2* knockout. Livers from experiments described in **E** were analyzed. Compare control and *Mst1/2* knockout groups, the change of all three target genes have a *P*-value < 0.001. Compare *Mst1/2* knockout with Mst1/2 knockout plus Ad-130a sp groups, the *P*-values for gene expression changes are as follows: CTGF, < 0.001; Cyr61, < 0.05; Inhba, < 0.01.

repressed (Figure 6C and Supplementary information, Figure S6B). To investigate the role of VGLL4 and miR-130a in YAP-induced liver tumorigenesis, we co-expressed YAP-5SA with VGLL4 or miR-130a. In YAP-5SA injected livers, small tumors were often obvious at day 70 (D70) after injection and several big tumors were often seen at D110 after injection (Figure 6D). However, co-expression of VGLL4 eliminated tumors at D70 and small tumors were only occasionally seen at D110 (Figure 6D). The lack of VGLL4 expression in these tumors suggested an origin from cells expressing only YAP-5SA (Supplementary information, Figure S6C). Thus VGLL4 markedly repressed YAP-induced liver tumorigenesis. In contrast, co-injection of YAP-5SA and pre-miR-130a induced not only small tumors but also numerous hyperplastic foci by D70 (Figure 6D). Consistently, these livers also showed much more tumors at D110 and some mice were moribund at the time (Figure 6D). Thus miR-130a promoted liver tumorigenesis induced by YAP.

It is well known that inactivation of the Hippo pathway increases organ size. Indeed, liver-specific *Mst1/2* knockout mediated by adenoviral Cre expression quickly led to liver enlargement within ten days (Figure 6E). Interestingly, the change of liver size and the induction of ectopic cell proliferation were blocked by co-injection of adenoviral miR-130a sponge (Figure 6E, 6F). Consistently, inhibition of miR-130a rescued VGLL4 protein level and abolished Hippo pathway target gene induction by *Mst1/2* knockout (Figure 6G). Taken together, the YAP-miR-130a-VGLL4 positive feedback loop plays a critical role in organ size regulation and tumorigenesis upon Hippo pathway deregulation.

bantam represses SdBP/Tgi protein level in Drosophila

The *Drosophila* VGLL4 homolog SdBP/Tgi also competes with Yki for Sd binding, thus regulates organ size [34, 44]. However, miR-130a is not conserved in *Drosophila*. To explore whether SdBP/Tgi might also be regulated by microRNAs, we used the PicTar microRNA target prediction algorithm. Unexpectedly, *bantam* is the best-predicted microRNA to target SdBP/Tgi in all six different *Drosophila* species analyzed, and a conserved *bantam*-binding site is present in the *SdBP/tgi* 3′UTR (Figure 7A). To test the functionality of this site, we made an *SdBP/tgi* 3′UTR sensor, which was inhibited by *bantam* to an extent similar to that of *hid* 3′UTR, a known *bantam* target [45] (Figure 7B). However, deletion of the *bantam*-binding site largely abrogated the repression (Figure 7B). This result strongly suggests that SdBP/Tgi is a target of *bantam*. Consistently, *bantam* mimic and *bantam* inhibitor diminished and elevated the protein levels of endogenous SdBP/Tgi in S2 cells, respectively (Figure 7C). To determine whether endogenous *bantam* regulates SdBP/Tgi protein level *in vivo*, we expressed the *bantam* sponge (*UAS-bantam.sp*) in *Drosophila* wing discs under the control of the *hh-Gal4* driver, which drives gene expression in the posterior compartments. As shown in Figure 7D, the *bantam.sp*-expressing compartment exhibited not only elevated *bantam* sensor GFP signal (panel II) but also increased SdBP/Tgi protein level (panel I, III). Furthermore, in *bantam* mutant ($Ban^{Δ1}$) clones generated by MARCM in wing discs, the protein level of SdBP/Tgi was increased (Figure 7E). Taken together, *bantam*, the *Drosophila* Yki target microRNA, has a function similar to mammalian miR-130a in repressing SdBP/Tgi protein level.

Discussion

Deregulation of the Hippo pathway leads to drastic change of organ size up to several folds in both *Drosophila* and mammals [46]. By contrast, alteration of other developmental pathways such as the insulin pathway alters organ size commonly within 50% [24]. In mammals, the regulation of organ size by the Hippo pathway depends on YAP transcriptional activity and TEADs [47]. However, YAP target genes are not only substantially different from Yki targets in *Drosophila*, but also vary among tissues and cells [3, 10, 12]. Notably, miR-29 has been identified as a YAP target gene mediating cross-talk with the mTOR pathway and affects cell size [48], suggesting that the mammalian Hippo pathway could function via microRNA targets. However, a functional microRNA mediating the organ size control activity of the mammalian Hippo pathway *in vivo* has not been pinpointed. Therefore, the robustness of the Hippo pathway has not been explained at the molecular level. In this study we identified a YAP-miR-130a-VGLL4 positive feedback loop (Figure 7F), which amplifies Hippo pathway signals thus sustaining potent transcriptional output and growth regulation.

In the previous model, the canonical Hippo pathway Mst1/2-Lats1/2 kinase cascade phosphorylates YAP causing its cytoplasmic retention and degradation [11, 12]. On the other hand, VGLL4 inhibits YAP further downstream at the level of TEAD binding [33, 34]. The two seemingly independent mechanisms could be complementary to each other as error-proof backups to put YAP activity in check. In this case, inactivation of the Hippo pathway should not be detrimental due to the presence of VGLL4. Apparently, this postulation is against the robust phenotypes of Hippo pathway inactivation. In our model, the Hippo pathway and VGLL4 activities are coordinated, with VGLL4 being a signal amplifier. The key in this

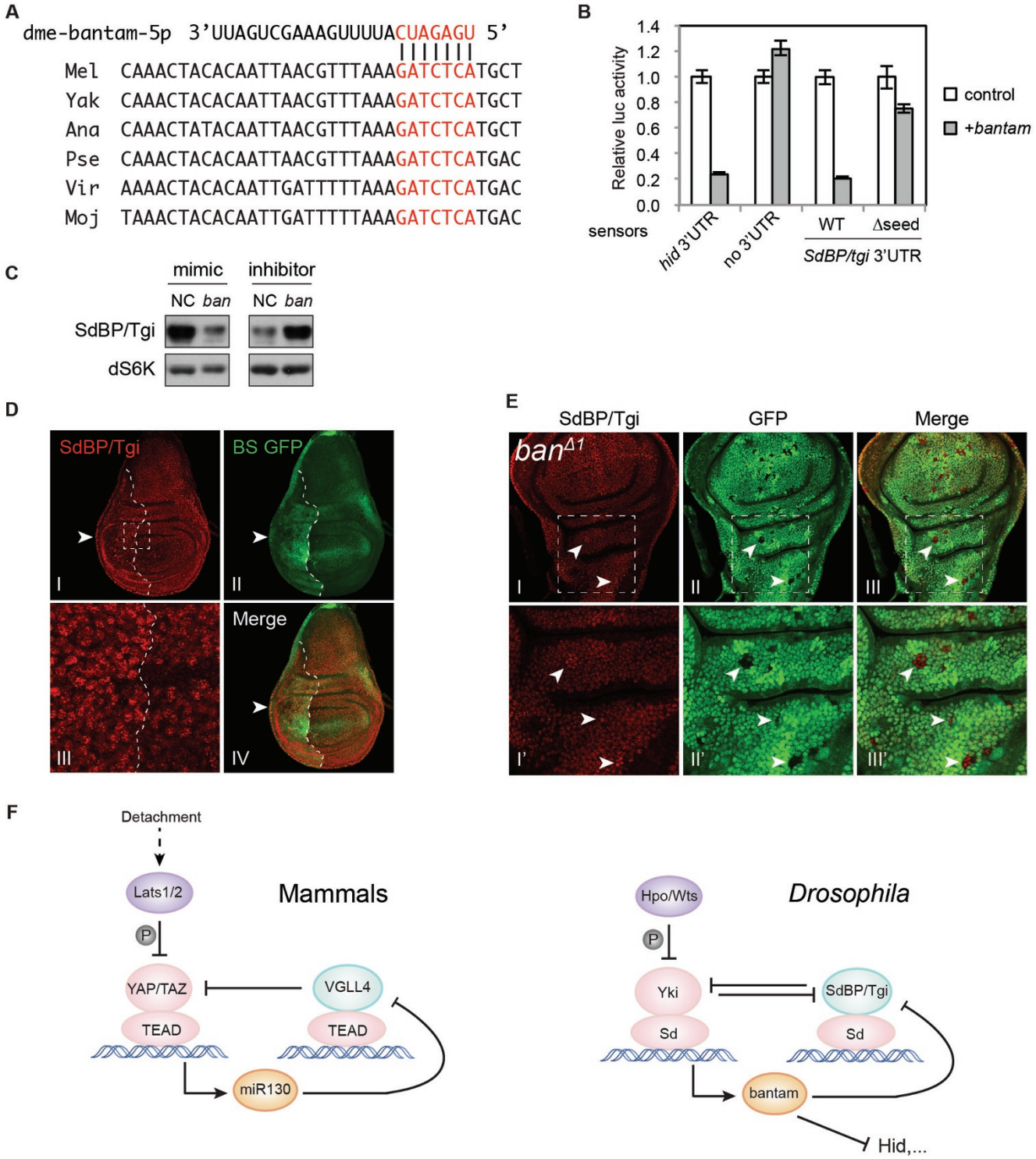

Figure 7 *bantam* represses SdBP/Tgi protein level in *Drosophila*. **(A)** Alignment indicates that *bantam*-seed-matching sequence in *SdBP/tgi* 3′UTR is conserved in different species of *Drosophila*. Matching nucleotides were labeled in red. **(B)** *SdBP/tgi* 3′UTR sensor is repressed by *bantam*. Indicated sensors were transfected into *Drosophila* S2 cells with or without *bantam* for luciferase assay. Experiments were performed in duplicates. **(C)** *bantam* mimic and inhibitor effect on SdBP/Tgi protein level. S2 cells were transfected and analyzed by immunoblotting. **(D)** Inhibition of *bantam* increases SdBP/Tgi protein level *in vivo*. Wing discs expressing *UAS-bantam.sp* in the P-compartment (indicated by arrowheads) under the control of *hhGal4* were subjected to immunostaining for SdBP/Tgi (red). The box in panel (I) is enlarged in panel (III). BS GFP (green) is the *bantam* sensor. **(E)** SdBP/Tgi protein level increases in *bantam* mutant clones in *Drosophila* wing discs. *bantam* mutant

(*Ban*$^{\Delta 1}$) clones were indicated by negative GFP (arrowheads). SdBP/Tgi protein levels were shown by immunostaining (red). Boxes in panels (I-III) were enlarged in (I′-III′). Fly genotype: *hsflp;;FRT80BubiGFP/FRT80BBan*$^{\Delta 1}$. **(F)** microRNA-mediated positive feedback loop of the Hippo pathway. Corresponding components in mammals and *Drosophila* were shown in the same color.

model is miR-130a, which puts VGLL4 under the control of the Hippo pathway and importantly, its upstream signals. Notably, although VGLL4 inhibits YAP-TEAD activity in both models, its role in the signaling circuit is fundamentally different and has not been clarified until this study.

Positive feedback loops are commonly seen in developmental pathways, which keep a developmental action silent in fluctuating background signals but trigger a robust response upon real stimuli at the right time and place. Although microRNAs are thought to be a mechanism as important as transcription regulators in mediating positive feedback loops [49], specific examples of microRNA-mediated circuits in major mammalian developmental pathways are few. Our study of miR-130a in the Hippo pathway provides such an example. By coupling the Hippo pathway phosphorylation signaling and the VGLL4 transcriptional repressor, miR-130a sustains the Hippo pathway output and a robust control of organ size. Our finding of miR-130a in a positive feedback loop also suggests its function in a context-dependent manner. In Hippo pathway inactive condition, miR-130a would be active providing a window for loss of function studies and potential therapeutic intervention. Such a mechanism may explain the lack of phenotypes for many other microRNA knockouts in normal condition [50], and highlights the importance of context in microRNA studies.

Interestingly, the finding of *Drosophila bantam* as an SdBP/Tgi repressor suggests that the positive feedback mechanism might be evolutionarily conserved (Figure 7F). This finding is unexpected because the nucleotide sequences of *bantam* and miR-130a are unrelated, which suggests that the logic of microRNA-mediated signaling circuits could be evolutionarily conserved independent of sequence. However, transcriptional regulation by the Hippo pathway in *Drosophila* might be more complicated than that in mammals as suggested by the absence of the potent YAP transcriptional activation domain in Yki. Indeed, it was recently suggested that Yki functions by relieving a default repression of Sd by SdBP/Tgi [34], although in situations such as *hippo* inactivation, the transcriptional activation activity of Yki itself plays a leading role. In the default repression model, *bantam* may mediate a coherent feedforward loop with a general structure: A (Yki in this case) inhibits C (SdBP/Tgi) and activates B (*bantam*), which is also a repressor of C (Figure 7F). Such a design is generally thought to improve fidelity of signaling circuits. In addition, *bantam* also inhibits apoptosis through repression of *hid* [45]. The exact molecular function of *bantam* in the *Drosophila* Hippo pathway might be context-dependent and awaits further investigation.

Numerous studies have demonstrated the oncogenic roles of YAP *in vitro* and *in vivo* [51]. More importantly, YAP activation has been found in human cancers such as HCC, neurofibromatosis 2 and uveal melanoma due to amplification of the *YAP* gene locus or mutations of *NF2* or *GNAQ*/*GNA11* [10, 28-32]. Furthermore, YAP is also a critical factor underlying tumor initiation and progression induced by other *bona fide* oncogenes such as *β-catenin* and *Kras* [52-54], suggesting a broader role of YAP in human cancers. In addition, TAZ has also been found elevated at protein level and genomically amplified in human cancers [29, 55]. Interestingly, TAZ was shown to confer breast cancer cells stem cell properties [56]. These findings have raised the therapeutic interest of YAP inhibition. Indeed, efficacy of inhibitors targeting YAP-TEAD interaction, such as verteporfin and the super-TDU peptide, has been demonstrated in uveal melanoma and gastric cancer models [31, 33, 47].

In this study, we show that miR-130a inhibition dampens Hippo pathway output and reverses organ size enlargement and tumorigenesis induced by Hippo pathway deregulation or YAP activation. These findings suggest miR-130a as a new target for anti-YAP therapy. Of note, miR-130a is also regulated by TAZ, although we did not further investigate the role of miR-130a in TAZ function. However, the similarity of YAP and TAZ in TEAD-binding suggests that TAZ activity may be regulated by miR-130a in a similar fashion. Importantly, technical breakthroughs on antisense microRNA oligomers (antimiRs) such as the application of nucleotide analogs, as well as acidic tumor microenvironment targeting technologies, have turned microRNAs into druggable targets of anti-cancer therapy with unique advantages [57, 58]. Thus our identification of the remarkable role of miR-130a in sustaining YAP activity would suggest modulating miR-130a as an exciting new approach for pharmacological intervention of cancer.

Materials and Methods

Antibodies, plasmids, mice and other materials

Information for materials is included in Supplementary infor-

mation, Data S1.

Cell culture, transfection and viral infection

Cell culture procedures are described in Supplementary information, Data S1.

Hydrodynamic injection

Male ICR mice of 4-week-old from Shanghai SLAC Laboratory Animal Company were used for injection. For each mouse, 50 μg of total transposon plasmids together with 10 μg of transposase-expressing plasmids were diluted in sterile Ringer's solution in a volume equal to 10% of body weight. The mixture was injected within 5 to 7 s through the tail vein.

Xenograft tumorigenesis model

Nude mice (nu/nu, male 6- to 8-week-old) were injected subcutaneously with 0.6-1 × 10^7 HepG2 stable cells. Around 3-4 weeks after injection, tumors were dissected and photographed.

Soft agar colony formation assay

About 2.5×10^4 cells were mixed with 3 ml growth medium containing 0.4% agarose and layered onto 2 ml of 0.75% agarose/medium beds in 6-well plates. Cells were fed with 2 ml growth medium every 3 days for 3 weeks, after which colonies were stained and counted.

Cell viability assay

One thousand cells were seeded in each well of 96-well microplates in triplicates. Cell viability was measured every other day using CellTiter-Blue assay kit (Promega) according to the manufacturer's instructions.

Anoikis assay

For anoikis analysis, cells were cultured in suspension for 48 h. Cells were then trypsinized and stained with PE Annexin V and analyzed by flow cytometry using the PE Annexin V Apoptosis Detection kit (BD Biosciences) following the manufacturer's instructions. Data were collected on a BD FACSCanto and analyzed using FlowJo software.

Luciferase assays

For promoter reporter and 3′UTR sensor luciferase assays, cells were transfected with the reporter, CMV-β-gal and indicated plasmids or microRNA mimics/inhibitors, and siRNAs. Thirty-six h after transfection, cells were lysed and luciferase activity was assayed using the Luciferase Assay System (Promega) following the manufacturer's instructions. All luciferase activities were normalized to β-galactosidase activity.

ChIP

ChIP assay was performed using the EZ-ChIP kit from Millipore according to the manufacturer's instructions. Briefly, cells were cross-linked, lysed and sonicated to generate DNA fragments with an average size of 0.5 kb. ChIP was performed using control IgG or 5 μg antibodies against Flag, YAP or TEAD1. IPs were then washed and eluted. The eluents were then de-crosslinked and DNA was purified for PCR analysis.

RNA isolation and real-time PCR

To determine the mRNA expression levels of regular genes and microRNA primary transcripts (pri-miRNAs), total RNA was isolated from cultured cells using Trizol reagent (Life Technologies). cDNA was synthesized by reverse transcription using random hexamers and subjected to real-time PCR with gene-specific primers in the presence of SYBR Green (Applied Biosystems). Relative abundance of mRNA was calculated by normalization to hypoxanthine phosphoribosyltransferase 1 mRNA.

microRNAs were extracted from cells using mirVana miRNA isolation kit (Life Technologies). The relative expression levels of microRNAs were determined using Taqman microRNA Assays (Life Technologies) normalized to RNU6B.

Detailed experimental procedures can be found in Supplementary information, Data S1.

Acknowledgments

We thank Drs Kun-Liang Guan and Ryan C Russell for critical reading of the manuscript; Fangtao Chi for help on preparing illustrations; Drs Zengqiang Yuan and Yingzi Yang for *Mst1/2* knockout mice; Dr Yong Cang for Albumin-Cre mice; Drs Tian Xu and Xiaohui Wu for the *piggyBac* system; Dr Zhaocai Zhou for gastric cancer cell lines and aliquots of VGLL4 antibody; Dr Stephen M Cohen for the *UAS-bantam.sp* and *Ban*^{A1} lines. Research in the lab of BZ is supported by grants from the State Key Development Program for Basic Research of China (2013CB945303), National Natural Science Foundation of China Excellent Yong Scholars Project (31422036), Natural Science Foundation of Zhejiang (LR12C07001), National Natural Science Foundation of China General Projects (31271508 and 31471316), Specialized Research Fund for the Doctoral Program of Higher Education (20130101110117), the 111 project (B13026), Fundamental Research Funds for Central Universities of China (2015XZZX004-17) and the Thousand Young Talents Plan of China.

References

1 Pan D. The hippo signaling pathway in development and cancer. *Dev Cell* 2010; **19**:491-505.
2 Yu FX, Guan KL. The Hippo pathway: regulators and regulations. *Genes Dev* 2013; **27**:355-371.
3 Dong J, Feldmann G, Huang J, *et al.* Elucidation of a universal size-control mechanism in *Drosophila* and mammals. *Cell* 2007; **130**:1120-1133.
4 Xin M, Kim Y, Sutherland LB, *et al.* Hippo pathway effector Yap promotes cardiac regeneration. *Proc Natl Acad Sci USA* 2013; **110**:13839-13844.
5 Cai J, Zhang N, Zheng Y, de Wilde RF, Maitra A, Pan D. The Hippo signaling pathway restricts the oncogenic potential of an intestinal regeneration program. *Genes Dev* 2010; **24**:2383-2388.
6 Heallen T, Morikawa Y, Leach J, *et al.* Hippo signaling impedes adult heart regeneration. *Development* 2013; **140**:4683-4690.
7 Chan EH, Nousiainen M, Chalamalasetty RB, Schafer A, Nigg EA, Sillje HH. The Ste20-like kinase Mst2 activates the human large tumor suppressor kinase Lats1. *Oncogene* 2005; **24**:2076-2086.
8 Callus BA, Verhagen AM, Vaux DL. Association of mammalian sterile twenty kinases, Mst1 and Mst2, with hSalvador

via C-terminal coiled-coil domains, leads to its stabilization and phosphorylation. *FEBS J* 2006; **273**:4264-4276.
9 Hergovich A, Schmitz D, Hemmings BA. The human tumour suppressor LATS1 is activated by human MOB1 at the membrane. *Biochem Biophys Res Commun* 2006; **345**:50-58.
10 Zhao B, Wei X, Li W, *et al.* Inactivation of YAP oncoprotein by the Hippo pathway is involved in cell contact inhibition and tissue growth control. *Genes Dev* 2007; **21**:2747-2761.
11 Zhao B, Li L, Tumaneng K, Wang CY, Guan KL. A coordinated phosphorylation by Lats and CK1 regulates YAP stability through SCF(beta-TRCP). *Genes Dev* 2010; **24**:72-85.
12 Hao Y, Chun A, Cheung K, Rashidi B, Yang X. Tumor suppressor LATS1 is a negative regulator of oncogene YAP. *J Biol Chem* 2008; **283**:5496-5509.
13 Lei QY, Zhang H, Zhao B, Zha ZY, Bai F, Pei XH, *et al.* TAZ promotes cell proliferation and epithelial-mesenchymal transition and is inhibited by the hippo pathway. *Mol Cell Biol* 2008; **28**:2426-2436.
14 Liu CY, Zha ZY, Zhou X, *et al.* The hippo tumor pathway promotes TAZ degradation by phosphorylating a phosphodegron and recruiting the $SCF^{\beta\text{-}TrCP}$ E3 ligase. *J Biol Chem* 2010; **285**:37159-37169.
15 Zhao B, Ye X, Yu J, *et al.* TEAD mediates YAP-dependent gene induction and growth control. *Genes Dev* 2008; **22**:1962-1971.
16 Zhang H, Liu CY, Zha ZY, *et al.* TEAD transcription factors mediate the function of TAZ in cell growth and epithelial-mesenchymal transition. *J Biol Chem* 2009; **284**:13355-13362.
17 Schlegelmilch K, Mohseni M, Kirak O, *et al.* Yap1 acts downstream of alpha-catenin to control epidermal proliferation. *Cell* 2011; **144**:782-795.
18 Yu FX, Zhao B, Panupinthu N, *et al.* Regulation of the Hippo-YAP pathway by G-protein-coupled receptor signaling. *Cell* 2012; **150**:780-791.
19 Miller E, Yang J, DeRan M, *et al.* Identification of serum-derived sphingosine-1-phosphate as a small molecule regulator of YAP. *Chem Biol* 2012; **19**:955-962.
20 Zhao B, Li L, Wang L, Wang CY, Yu J, Guan KL. Cell detachment activates the Hippo pathway via cytoskeleton reorganization to induce anoikis. *Genes Dev* 2012; **26**:54-68.
21 Dupont S, Morsut L, Aragona M, *et al.* Role of YAP/TAZ in mechanotransduction. *Nature* 2011; **474**:179-183.
22 Wada K, Itoga K, Okano T, Yonemura S, Sasaki H. Hippo pathway regulation by cell morphology and stress fibers. *Development* 2011; **138**:3907-3914.
23 Sansores-Garcia L, Bossuyt W, Wada K, *et al.* Modulating F-actin organization induces organ growth by affecting the Hippo pathway. *EMBO J* 2011; **30**:2325-2335.
24 Leevers SJ, McNeill H. Controlling the size of organs and organisms. *Curr Opin Cell Biol* 2005; **17**:604-609.
25 Overholtzer M, Zhang J, Smolen GA, *et al.* Transforming properties of YAP, a candidate oncogene on the chromosome 11q22 amplicon. *Proc Natl Acad Sci USA* 2006; **103**:12405-12410.
26 Zhou D, Conrad C, Xia F, *et al.* Mst1 and Mst2 maintain hepatocyte quiescence and suppress hepatocellular carcinoma development through inactivation of the Yap1 oncogene. *Cancer Cell* 2009; **16**:425-438.
27 Zhou D, Zhang Y, Wu H, *et al.* Mst1 and Mst2 protein kinases restrain intestinal stem cell proliferation and colonic tumorigenesis by inhibition of Yes-associated protein (Yap) overabundance. *Proc Natl Acad Sci USA* 2011; **108**:E1312-1320.
28 Zender L, Spector MS, Xue W, *et al.* Identification and validation of oncogenes in liver cancer using an integrative oncogenomic approach. *Cell* 2006; **125**:1253-1267.
29 Song Y, Li L, Ou Y, *et al.* Identification of genomic alterations in oesophageal squamous cell cancer. *Nature* 2014; **509**:91-95.
30 Feng X, Degese MS, Iglesias-Bartolome R, *et al.* Hippo-independent activation of YAP by the GNAQ uveal melanoma oncogene through a trio-regulated rho GTPase signaling circuitry. *Cancer Cell* 2014; **25**:831-845.
31 Yu FX, Luo J, Mo JS, *et al.* Mutant Gq/11 promote uveal melanoma tumorigenesis by activating YAP. *Cancer Cell* 2014; **25**:822-830.
32 Zhang N, Bai H, David KK, *et al.* The Merlin/NF2 tumor suppressor functions through the YAP oncoprotein to regulate tissue homeostasis in mammals. *Dev Cell* 2010; **19**:27-38.
33 Jiao S, Wang H, Shi Z, *et al.* A peptide mimicking VGLL4 function acts as a YAP antagonist therapy against gastric cancer. *Cancer Cell* 2014; **25**:166-180.
34 Koontz LM, Liu-Chittenden Y, Yin F, *et al.* The hippo effector yorkie controls normal tissue growth by antagonizing scalloped-mediated default repression. *Dev Cell* 2013; **25**:388-401.
35 Zhang W, Gao Y, Li P, *et al.* VGLL4 functions as a new tumor suppressor in lung cancer by negatively regulating the YAP-TEAD transcriptional complex. *Cell Res* 2014; **24**:331-343.
36 Thompson BJ, Cohen SM. The Hippo pathway regulates the bantam microRNA to control cell proliferation and apoptosis in *Drosophila*. *Cell* 2006; **126**:767-774.
37 Nolo R, Morrison CM, Tao C, Zhang X, Halder G. The bantam microRNA is a target of the hippo tumor-suppressor pathway. *Curr Biol* 2006; **16**:1895-1904.
38 Huang H, Li J, Hu L, *et al.* Bantam is essential for *Drosophila* intestinal stem cell proliferation in response to Hippo signaling. *Dev Biol* 2014; **385**:211-219.
39 Song H, Mak KK, Topol L, *et al.* Mammalian Mst1 and Mst2 kinases play essential roles in organ size control and tumor suppression. *Proc Natl Acad Sci USA* 2010; **107**:1431-1436.
40 Lu L, Li Y, Kim SM, *et al.* Hippo signaling is a potent *in vivo* growth and tumor suppressor pathway in the mammalian liver. *Proc Natl Acad Sci USA* 2010; **107**:1437-1442.
41 McClatchey AI, Saotome I, Mercer K, *et al.* Mice heterozygous for a mutation at the Nf2 tumor suppressor locus develop a range of highly metastatic tumors. *Genes Dev* 1998; **12**:1121-1133.
42 Lee KP, Lee JH, Kim TS, *et al.* The Hippo-Salvador pathway restrains hepatic oval cell proliferation, liver size, and liver tumorigenesis. *Proc Natl Acad Sci USA* 2010; **107**:8248-8253.
43 Tao J, Calvisi DF, Ranganathan S, *et al.* Activation of beta-catenin and Yap1 in human hepatoblastoma and induction of hepatocarcinogenesis in mice. *Gastroenterology* 2014; **147**:690-701.
44 Guo T, Lu Y, Li P, *et al.* A novel partner of Scalloped regulates Hippo signaling via antagonizing Scalloped-Yorkie activity. *Cell Res* 2013; **23**:1201-1214.

45 Brennecke J, Hipfner DR, Stark A, Russell RB, Cohen SM. Bantam encodes a developmentally regulated microRNA that controls cell proliferation and regulates the proapoptotic gene hid in *Drosophila*. *Cell* 2003; **113**:25-36.
46 Zhao B, Li L, Lei Q, Guan KL. The Hippo-YAP pathway in organ size control and tumorigenesis: an updated version. *Genes Dev* 2010; **24**:862-874.
47 Liu-Chittenden Y, Huang B, Shim JS, *et al.* Genetic and pharmacological disruption of the TEAD-YAP complex suppresses the oncogenic activity of YAP. *Genes Dev* 2012; **26**:1300-1305.
48 Tumaneng K, Schlegelmilch K, Russell RC, *et al.* YAP mediates crosstalk between the Hippo and PI(3)K-TOR pathways by suppressing PTEN via miR-29. *Nat Cell Biol* 2012; **14**:1322-1329.
49 Ebert MS, Sharp PA. Roles for microRNAs in conferring robustness to biological processes. *Cell* 2012; **149**:515-524.
50 Vidigal JA, Ventura A. The biological functions of miRNAs: lessons from *in vivo* studies. *Trends Cell Biol* 2015; **25**:137-147.
51 Moroishi T, Hansen CG, Guan KL. The emerging roles of YAP and TAZ in cancer. *Nat Rev Cancer* 2015; **15**:73-79.
52 Kapoor A, Yao W, Ying H, *et al.* Yap1 activation enables bypass of oncogenic Kras addiction in pancreatic cancer. *Cell* 2014; **158**:185-197.
53 Shao DD, Xue W, Krall EB, *et al.* KRAS and YAP1 converge to regulate EMT and tumor survival. *Cell* 2014; **158**:171-184.
54 Rosenbluh J, Nijhawan D, Cox AG, *et al.* β-Catenin-driven cancers require a YAP1 transcriptional complex for survival and tumorigenesis. *Cell* 2012; **151**:1457-1473.
55 Chan SW, Lim CJ, Guo K, *et al.* A role for TAZ in migration, invasion, and tumorigenesis of breast cancer cells. *Cancer Res* 2008; **68**:2592-2598.
56 Cordenonsi M, Zanconato F, Azzolin L, *et al.* The Hippo transducer TAZ confers cancer stem cell-related traits on breast cancer cells. *Cell* 2011; **147**:759-772.
57 Chen Y, Gao DY, Huang L. *In vivo* delivery of miRNAs for cancer therapy: challenges and strategies. *Adv Drug Deliv Rev* 2015; **81**:128-141.
58 Cheng CJ, Bahal R, Babar IA, *et al.* MicroRNA silencing for cancer therapy targeted to the tumour microenvironment. *Nature* 2015; **518**:107-110.

(**Supplementary information** is linked to the online version of the paper on the *Cell Research* website.)